

Modeling the global inter-annual variability of ozone due to the equatorial QBO and to extra-tropical planetary wave variability.

Jonathan S. Kinnersley
and
Ka Kit Tung

Department of Applied Math,
University of Washington,
Seattle WA 98195-2420

Submitted: February 1997
Revised: September 1997

Abstract

By forcing an interactive chemical–dynamical model of the stratosphere with the observed Singapore zonal winds and with the observed daily–varying planetary wave heights just above the tropopause over the period from March 1980 to February 1993 much of the observed inter–annual variability (IAV) in the monthly–mean ozone column from pole to pole was able to be reproduced. The best correlations were obtained equatorwards of 50 degrees during winter and autumn in both hemispheres. These correlations were due to the model’s interaction with the specified equatorial zonal wind. In the southern hemisphere (SH), the observed high latitude ozone anomaly in November (the month with the largest anomaly) is well anti–correlated with the 20mb Singapore wind, and correlations suggest the anomaly propagates polewards from 45°S in August and possibly even from 15°S in June. The model reproduces this behaviour well. In the northern hemisphere (NH) by contrast the observed high latitude ozone anomaly is not well correlated with the equatorial QBO nor does it propagate from lower latitudes. Model results demonstrate that the NH high latitude ozone anomaly is influenced strongly by the IAV in the forcing of the planetary waves. Model results show a large IAV in the ozone column during polar night in the NH (where TOMS is not able to observe) which is due to the IAV in the forcing of planetary waves.

1 Introduction

There is a significant amount of interannual variability (IAV) in the monthly-mean zonal-mean ozone column, and a considerable amount of effort has been spent in trying to understand its causes. While a large part of the variability over the past decade (especially at high southern latitudes) is a negative trend due to the increase in the chlorine loading of the stratosphere, much of it is also due to natural variability and it is important to be able to separate the causes of the observed IAV. This paper will focus on two sources of natural variability – the equatorial quasi-biennial oscillation (QBO) in zonal wind and the variability in the forcing of stratospheric planetary waves at the tropopause. The former has been studied fairly extensively already, using both observations (eg. Hasebe 1984, Bowman 1989, Lait et al. 1989, Randel and Cobb 1994, Tung and Yang 1994a, Hollandsworth et al. 1995, Randel and Wu 1996, Sitnov 1996) and models (eg. Gray and Pyle 1989, Gray and Ruth 1993, Tung and Yang 1994b) but the importance of the latter to the ozone column has not yet been quantified, though its effect on the stratospheric zonal wind in the northern hemisphere (NH) was estimated, using an interactive model, by Kinnersley (1998).

The QBO signal in extra-tropical ozone was at first (eg. Hasebe 1984, Lait et al. 1989) analysed without considering in depth the interaction between the tropical QBO and the stratospheric circulation’s seasonal cycle. Subsequently, the seasonal synchronisation of the subtropical ozone QBO anomaly was noted by Bowman (1989) and Hamilton (1989) and modeled by Gray and Dunkerton (1990) and Gray and Ruth (1993) using a two-dimensional model. In addition, Tung and Yang (1994a) highlighted the fact that the middle and high-latitude ozone variability seemed to involve an interference between the approximately 30 month tropical QBO and the 12 month seasonal cycle. They used a simplified model (Tung and Yang 1994b) to demonstrate their results, and assumed that the tropical QBO somehow modulated the extra-tropical planetary wave forcing in winter (as suggested in earlier studies by Holton and Tan (1982) and Dunkerton and Baldwin (1991)) and hence the meridional circulation, so that the extra-tropical ozone variation was mainly a manifestation of the circulation anomaly in the extra-tropics. In their model the extra-tropical anomaly in column ozone was created locally, with high column ozone in regions of enhanced downwards transport and low column ozone in regions of enhanced upwelling. This is a different and perhaps complimentary view to the one suggested by Gray and Pyle (1989), who modeled an extra-tropical QBO in ozone by a polewards advection and diffusion of the tropical anomaly. It would be useful to use a more realistic model with an interaction between planetary waves and the mean flow to see to what extent the observed extra-tropical ozone anomaly can be reproduced. Also, a more complicated model would be able to use the information contained in the tropical wind at all levels, rather than assuming that the tropical QBO can be represented simply by the wind at a single pressure level, as has been done in previous observational and modeling studies (though Randel and Wu (1996) found that a linear combination of the Singapore winds was better correlated with the observed ozone column than the wind at a single level). Such a modeling approach was taken previously by Gray and Ruth (1993), but their model did not simulate the interaction between planetary waves and the zonal-mean wind. Chipperfield et al. (1994) used a model (an earlier version of the model used in this study) with such an interaction, but little attention was paid to the extra-tropical variability.

In the SH, a strong QBO signal has been found at high latitudes (eg. Garcia and Solomon 1987, Lait et al 1989, Randel and Cobb 1994). The high latitude NH QBO signal is, however, weaker than that of the SH (see eg. Randel and Cobb 1994, Yang and Tung 1994a). It is probable that variability in planetary wave forcing from the lower stratosphere in the NH (which may be influenced by a number of factors, such as wave propagation from the troposphere, or the equatorial QBO) is important to the high-latitude ozone column variability. That it is important to the variability of the 10mb zonal winds was demonstrated by Kinnersley (1998) using the same model used in this paper. It might be difficult to find a quantity related to the wave activity in the lower stratosphere which is well correlated with the high-latitude ozone column variability. Also, merely finding correlations would not demonstrate a causal link, but only suggest it. An alternative to looking for correlations is to feed the planetary wave amplitudes observed just above the tropopause into an interactive model which is able to calculate the resultant planetary waves throughout the stratosphere as well as their interaction with the zonal-mean state and estimate the resultant variability induced in the ozone column. That is the approach taken in this study, with waves on the 368K isentropic level being used (which lies near the 150mb surface, just above the extra-tropical tropopause).

The model and data used here will be described in section 2. Then in section 3 the correlation of the observed ozone column with the Singapore wind will be presented and discussed with respect to previous studies. The model runs will be presented in section 4, and the results will be discussed in the concluding section.

2 Model, Data and statistics.

2.1 Model

The model used here is the ‘THIN AIR’ model with zonally truncated dynamics and zonally-averaged chemical and radiative modules. It is described fully in Kinnersley (1996). It has 19 horizontal boxes from pole to pole and 29 levels in the vertical, from the ground to about 100km. It uses an explicit Adams-Bashford time-integration with a step of 2 hours. However, unlike the model version used in Kinnersley (1996), in the version used here the planetary wave breaking parametrisation has been replaced by a meridional diffusion of wave potential vorticity with a constant diffusion coefficient which damps 2-grid-length scale anomalies with an e-folding time of about 10 days. Also, the planetary waves were damped within 27 degrees of the equator with a time-constant of 1.5 days since it was shown in Kinnersley (1998) that this led to a better simulation of the interannual variability in the zonal wind during late winter in the NH. Similar results were obtained using the original breaking parametrisation, but it was decided to use the simpler scheme here to show that the results do not depend strongly on the kind of wave-breaking parametrisation used. The meridional diffusion coefficient for trace gases in the model is parametrised by the flux-gradient method of Tung (1986) and Yang et al. (1990) and depends on the ratio of Ertel’s potential vorticity (PV) flux to the meridional gradient of the zonal-mean PV. This method assumes that the main cause of a non-zero time-averaged PV flux is a meridional diffusion of eddy PV. This is indeed true for this model, so it seems appropriate to use it here. This method has the

following limitation, however. Provided the zonal-mean meridional PV gradient is positive (which is true most of the time) the method results in a diffusion coefficient whose sign is opposite to that of the PV flux. A reversible wave vacillation will result in negative and positive PV fluxes as the wave grows and then decays, and hence positive and negative values of diffusion coefficient. Over the whole vacillation the net diffusion should be zero (if the vacillation is reversible). However, the problem with this method is that it will overestimate the diffusion for the simple reason that the numerical model cannot handle negative diffusion coefficients and has to set them equal to zero. This problem would not be so acute if the time-mean diffusion were parametrised in terms of the time-mean PV flux (as was done in Yang et al. 1990, for example), but that cannot be done in this model, which computes the daily evolution of the stratosphere. With this in mind, extra model runs were carried out, one with this parametrised diffusion and one with zero diffusion so that the uncertainty in the modeled results might be quantified. The results obtained while using the parametrised diffusion were very similar to those obtained while using no diffusion, but were in general more realistic. Therefore, only results from the runs with diffusion will be discussed in this paper.

A simple gravity wave parametrisation helps to produce realistic upper stratospheric and mesospheric winds, and also determines the vertical diffusion of trace gases in the stratosphere using Lindzen’s (1981) technique. Near the tropopause a value of $1\text{m}^2\text{s}^{-1}$ is used to represent cross-tropopause diffusion.

The planetary-wave module solves the quasi-geostrophic system of equations for the three longest zonal wave components (that is, it integrates the prognostic equations for the wave components of Ertel’s PV using the geostrophic winds derived by inverting PV at each time step) and includes wave-wave interactions as well as interactions with the modeled zonal-mean state. Its bottom boundary is the 368K isentropic surface (which lies near 150mb) and its waves are forced there with the observed daily wave heights expressed in terms of the Montgomery potential. For the runs described in this paper, with the exception of one control run, the model’s planetary waves in the NH were forced at the 368K isentropic surface using the observed planetary wave amplitudes from March 1980 to February 1993. In the SH the forcing of the waves on the 368K surface was annually periodic (using the daily-varying data from July 1980 to June 1981) since use of the observed interannually-varying waves gave unrealistic results in the modeled SH. This may be due to errors in the observations, which rely on a sparse set of observations of surface pressure in the SH to build up the geopotential height data throughout the atmosphere. In addition, with the exception of a second control run, the zonal winds in the model between 10mb and 70mb and equatorwards of 10 degrees north and south were relaxed towards the observed Singapore wind with a time constant of 1 day, similar to Chipperfield et al. (1994).

Holton and Mass (1976) suggested that the stratosphere may be chaotic, even with a constant forcing from the troposphere but it was shown in Kinnersley (1998) that the model used here is not chaotic in this way.

2.2 Data

The ozone values came from the Total Ozone Mapping Spectrometer (TOMS) data set (version 7) from November 1978 to April 1993. The ozone data was detrended using a

least-squares fit to determine the trend. The daily planetary-wave heights used to force the model's waves were derived from National Meteorological Center data from March 1980 to February 1993.

2.3 Statistics

The correlations shown throughout this paper are all calculated from monthly-mean values. The significance of the correlations was estimated in the following simple way. The correlation between, for example, the observed and modeled anomalies in the monthly-mean ozone column at a certain latitude from 1980 to 1992 involves 13 pairs of numbers. With 13 pairs of random numbers, the probability of obtaining a correlation coefficient of greater than 0.48, 0.64 and 0.79 is 0.05, 0.01 and 0.001 respectively. This is expressed in this paper by saying that correlations of 0.48, 0.64 and 0.79 obtained over 13 years are significant at the 95% , 99% and 99.9% levels respectively. The standard deviations referred to in the text are the standard deviations of the monthly-mean, zonal-mean value from the average value (over the entire data record) for that month.

3 Correlation of ozone column with Singapore wind

A number of methods have been used to isolate a signal in the global ozone column which is correlated with the equatorial QBO in stratospheric zonal wind. Chandra and Stolarski (1991) showed the correlation between the 30mb Singapore wind and the TOMS ozone column from 60S to 60N and for each month of the year, and also calculated a regression coefficient. This revealed the seasonal dependence of the QBO signal in ozone, which was clearly strongest during winter and autumn. Bowman (1989), Hollandsworth et al. (1995) and Sitnov (1996) calculated lagged correlations and anomalies of ozone with the Singapore wind at a certain level, with positive and negative lags of up to two years. While these revealed a significant QBO signal even at high latitudes, they hid its seasonality.

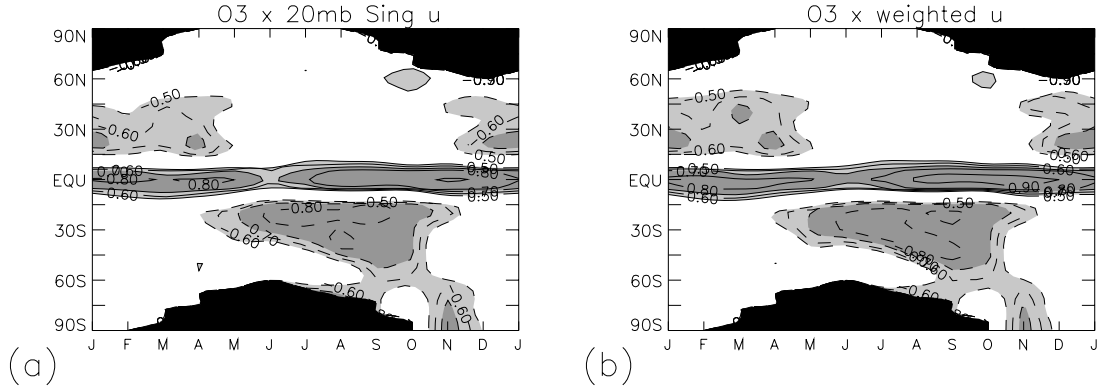


Figure 1: *Correlation of observed ozone column anomaly (detrended and deseasonalised) from March 1980 to February 1993 with (a) the 20mb Singapore zonal wind and (b) with Randel and Wu's (1996) linear combination of the Singapore winds. Contours at $\pm 0.5, \pm 0.6, \dots$, negative contours dashed, absolute values greater than 0.5 lightly shaded, absolute values greater than 0.7 more heavily shaded. The polar night is blacked out.*

Since we are interested here in the seasonality of the extra-tropical ozone QBO the zero-lagged correlation of the detrended TOMS ozone column from March 1980 till February 1993 with the 20mb Singapore wind is shown in figure 1a. The 13 year time span used here is shorter than the total TOMS record, but it is used in order to be able to compare it with the model results. However, there is no reason to suppose that the extra-tropical QBO signal should depend solely on the Singapore wind at one particular level, and Randel and Wu (1996) found a linear combination of the Singapore winds from 10mb to 70mb which provided a better fit to the ozone variability than the wind at a single level. Therefore, for comparison, the correlation with Randel and Wu's (1996) linear combination of winds (in which the 20mb wind received the strongest weighting) is shown in figure 1b. Although use of the linear combination of winds does give slightly better results over the equator and near 45N from November till April, on the whole the results are very similar to those obtained using the 20mb wind alone. Strong correlations in figure 1 are obtained near the equator for all months of the year, which is consistent with theory and previous studies. There is a node at about 10 degrees north and south where the correlation with the equatorial wind changes sign. In the SH there is a strong negative correlation which starts in March and extends from about 10S to 30S and which then grows in width till it extends from 10S to about 50S in October. In the NH the correlation is again strongest in winter and spring, but is not as strong as in the SH, nor does it spread with time away from the tropics. It also starts later in the seasonal cycle – in early winter as opposed to late autumn in the SH.

The NH high latitude (north of 50N) winter and spring ozone column does not seem to be strongly influenced by the Singapore winds. However, in the SH in November there is a significant high-latitude ozone column modulation by the 20mb Singapore wind. This inter-hemispheric difference (a weaker NH QBO signal) is also present in Randel and Cobb's (1994) results. This is the opposite of what was found by Hollandsworth et al. (1995), who saw a stronger QBO signal at NH high latitudes than at high latitudes in the SH. Although

the difference is presumably due to the latter's use of lagged correlations, it is not clear to us why the difference arises.

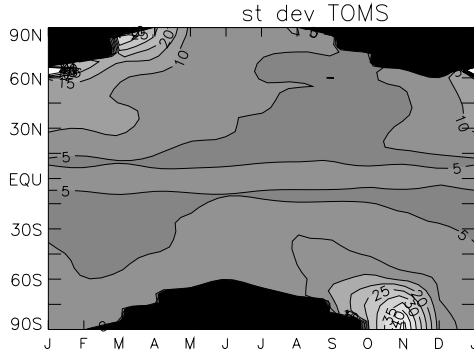


Figure 2: *Standard deviation of the observed ozone column anomaly (detrended and deseasonalised) from March 1980 to February 1993 (contours every 5 DU).*

From figure 1 it seems that the SH ozone column anomaly may be propagating from low latitudes in June to high latitudes in November, while such a propagation is not evident in the NH. This difference between the NH and SH at high latitudes can be further revealed by calculating the correlation between the high latitude ozone column anomaly of a certain month and the low latitude ones over the preceding 12 months. The standard deviation of the monthly-mean ozone column at 60S is largest in November and at 60N it is largest in February (figure 2) so these are the two high latitude points we shall use. The correlation between the anomaly at 60S in November and the anomaly at every latitude over the preceding 12 months (figure 3a) suggests a strong propagation of the anomaly from 15S in June (correlation of 0.6) to 45S in August (correlation of 0.8) and eventually to 60S in November.

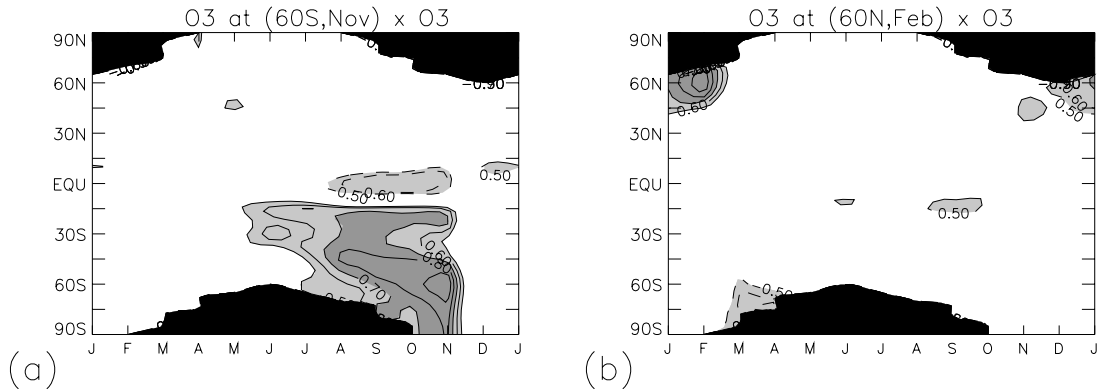


Figure 3: (a) Correlation of observed ozone column anomaly (detrended and deseasonalised) at 60S in November with observed anomaly at all latitudes over the preceding 12 months. (b) as (a) but using the anomaly at 60N in February. Contours and shading as figure 1.

If the anomalies at these three points in time and latitude were random, the chance of finding correlations of 0.64 and 0.79 would be 1% and 0.1% respectively, so it would seem that these anomalies are not random but are linked together, possibly by polewards advection or diffusion. The corresponding calculation for the NH (figure 3b), correlating the anomaly at 60N in February with that over the preceding 12 months, suggests no propagation of the anomaly from lower latitudes. This is consistent with the work of Yang and Tung (1995), who found no phase propagation of the ozone QBO in the NH.

It will be argued in section 4 that the weaker NH high latitude QBO signal found in this study, and the isolation of the NH winter high latitude ozone anomaly, are due to the disruption of the QBO signal by the variability in the forcing of the NH planetary waves.

4 Results of model runs

Three model runs will be presented in this section. In Run A the model is forced both by the equatorial Singapore winds from 10mb to 70mb and by the observed NH wave amplitudes on the 368K isentropic surface from March 1980 to February 1993. In the SH the forcing of the waves on the 368K surface was annually periodic (see section 2). The model was initialised using the March values from the final year of a 12-year run where the forcing of the model's planetary waves at the 368K surface was made annually periodic in both hemispheres by repeating the observed wave heights from July 1980 to June 1981. Two control runs, in which these two forcings were applied separately, will be described in sections 4.2 and 4.3.

4.1 Run A – with equatorial QBO and variable forcing of NH planetary waves.

The model was run as described above for 13 years using the observed forcings from March 1980 to February 1993.

The performance of the model was shown in Kinnersley (1996) to be very realistic in a number of ways, but since the model is slightly different in this study, and is run with forcings which vary from year to year, the 13-year average of the modeled and observed ozone columns are shown for comparison in figure 4.

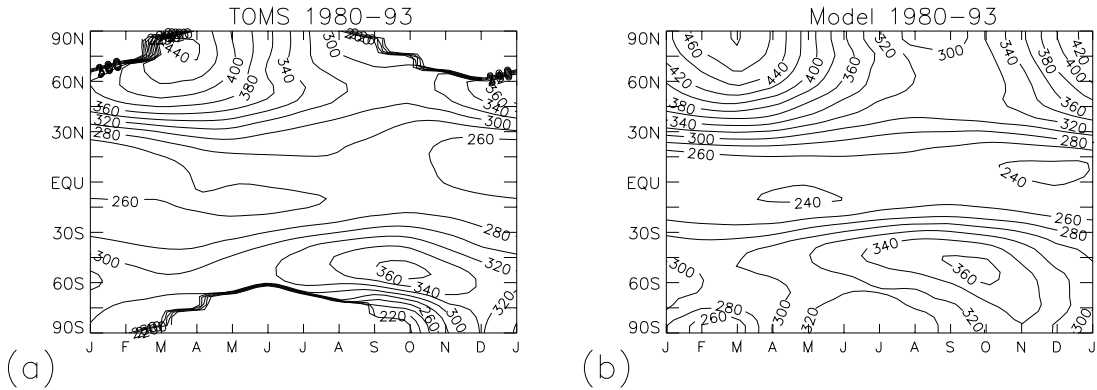


Figure 4: 13-year average (1980-1992) of ozone column (a) from TOMS data (b) from model.

The model generally compares well with observations, when it is taken into account that the chlorine loading in the model is held close to the value estimated for 1980. The model is therefore unable to reproduce the severe ozone losses observed after 1985 at the south pole in October.

For comparison with Tung and Yang (1994b), and for a general picture of the model's performance, the modeled and observed ozone columns at certain latitudes for each month from January 1982 to December 1992 are plotted in figure 5.

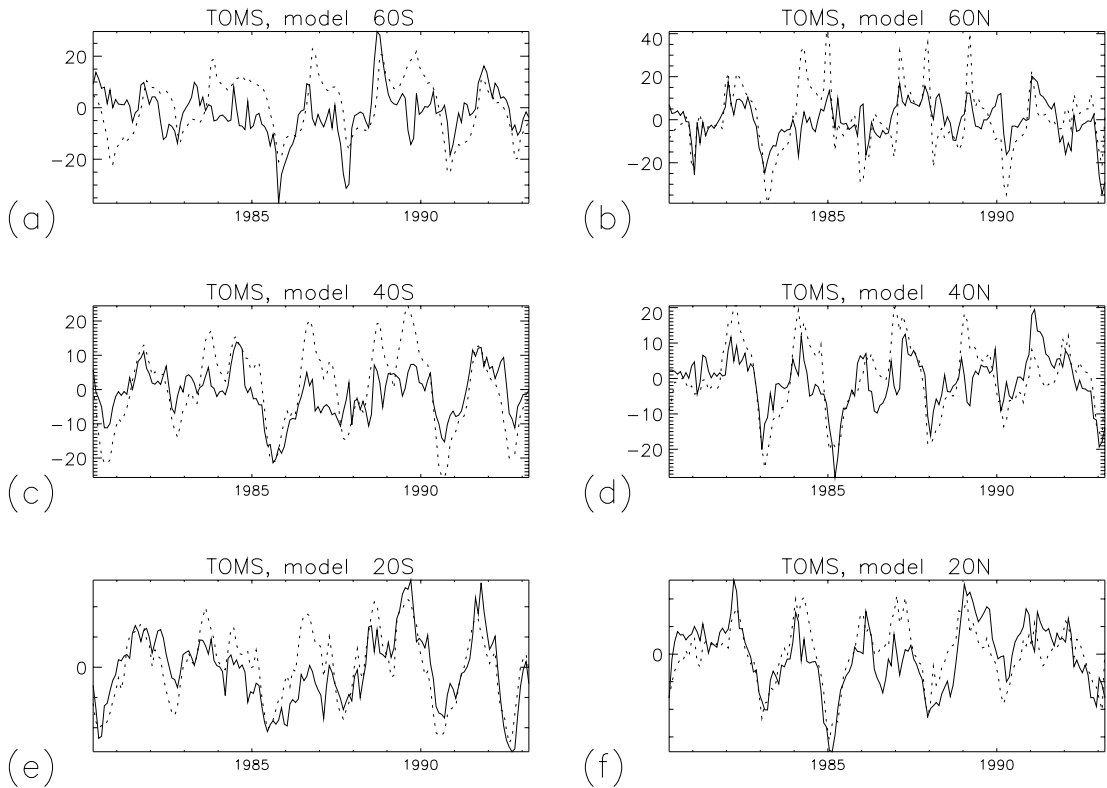


Figure 5: Comparison of modeled (dashed) and observed (solid) ozone column anomalies (detrended and deseasonalised) from Mar 1980 to Feb 1993 at (a) 60S (b) 60N (c) 40S (d) 40N (e) 20S (f) 20N.

In general the model is quite close to observations. At 60N the modeled anomaly is somewhat larger than observed – this will be discussed later. Also, the model’s anomalies tend to spread over a wider latitude range than observed. For example, the modeled positive anomaly at 20S in mid 1989 travels to 60S in late 1989 and even grows, whereas the observed anomaly at 20S is not apparent at 40S or 60S. This is more evident in the contour plot of both anomalies (see figure 6), where the smoothness of propagation of the modeled SH anomaly is contrasted with the much more noisy TOMS data.

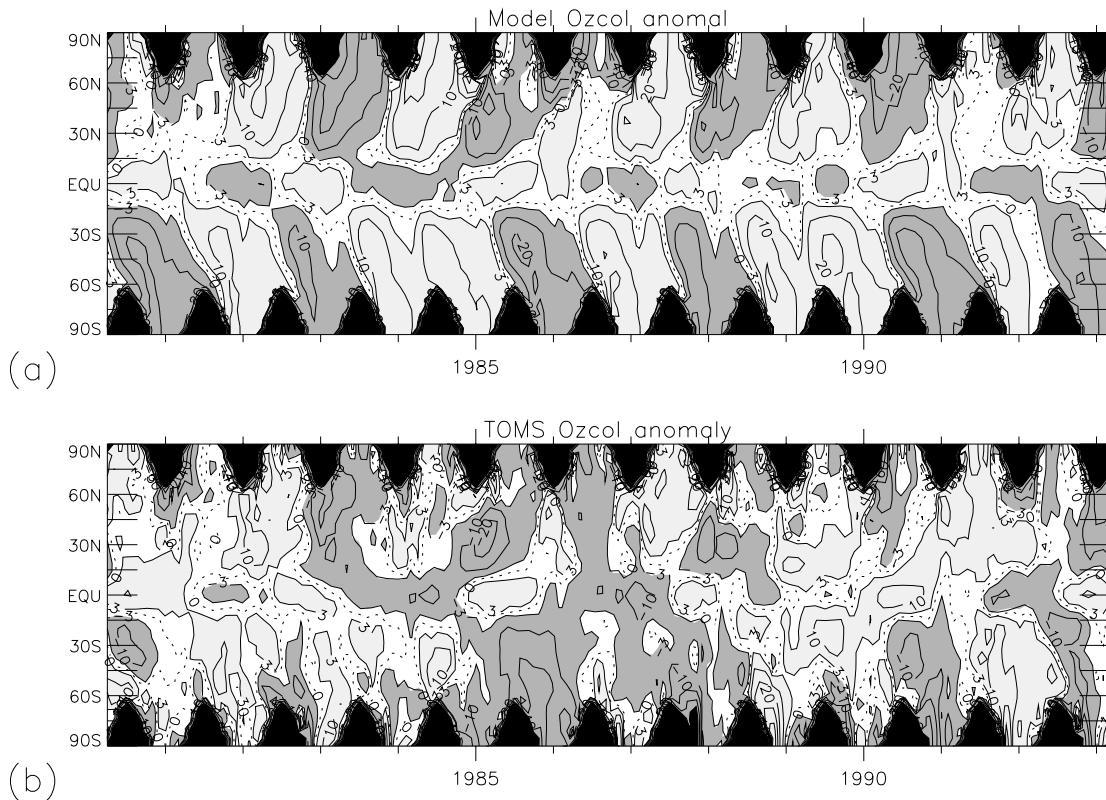


Figure 6: Ozone column anomaly from (detrended and deseasonalised) (a) full model and (b) TOMS data. Contours at 0, ± 3 , ± 10 , ± 20 , ± 40 , ± 60 DU. Values above 3 shaded.

Yang and Tung (1995) noted that the observed ozone column in the NH changes sign near 55N during some winters. They speculated that this may be caused by interannual variability in the high latitude planetary waves, since they were unable to reproduce the sign change in their simple model incorporating only equatorial QBO variability. This feature is now reproduced in the NH of this model (see figure 6), in particular in the early winters of 1984/5, 1987/8 and 1991/2, though a better comparison is hindered by lack of observations during polar night. It must be borne in mind that the model’s horizontal resolution of 9

degrees limits the precision of the comparison. Note also that the model's NH is more noisy than the SH, due to the interannual variability in the 368K wave heights in the NH. This makes the model's NH look more realistic than its SH, and suggests that although the model mimics the observed SH ozone anomaly well in general (see later), interannual variability in the SH planetary wave forcing at a level in the lower stratosphere may be the cause of the observed noise in the SH ozone column anomaly. The polar night regions have been blacked out in the model results for an easier comparison with TOMS data. The depletion of ozone during the NH winters of 1992 and 1993 in the TOMS data (analysed by Randel and Wu (1996), among others) is evident from a comparison between modeled and observed anomalies.

The correlation of modeled with observed ozone anomalies shown in figure 7(a) is a critical test of the model since the correlation is calculated at each latitude and month over the 13 year period.

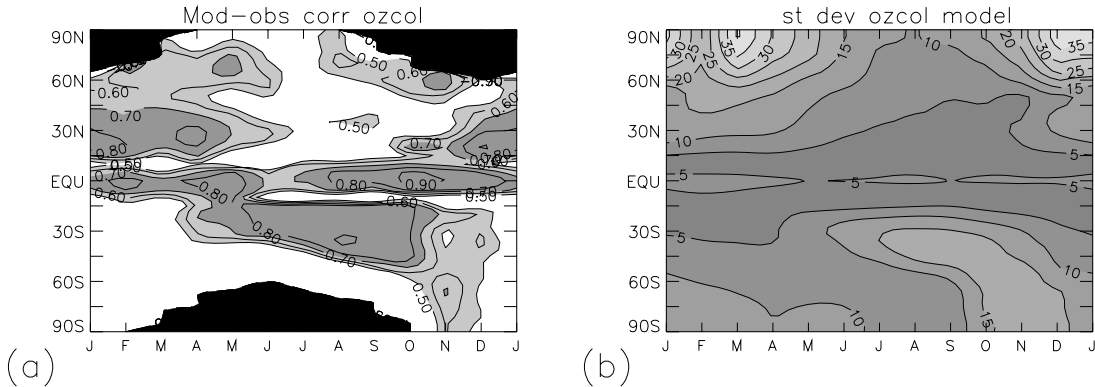


Figure 7: (a) Correlation of modeled and observed ozone column anomalies (detrended and deseasonalised) from Mar 1980 to Feb 1993. Contours and shading as in figure 1. (b) Standard deviation of the modeled ozone column anomaly.

As expected, the correlation is strong equatorwards of 10 degrees since the model zonal winds are specified from observations there. It is also strong between about 10 and 50 degrees in both hemispheres during their respective winters and springs, which is when the wave induced polewards circulation is strong. The model's variability at mid-latitudes (see figure 7b) is somewhat larger than observed, however. The reason for this is at present unclear.

In the NH, the correlation between the high latitude modeled and observed ozone column anomalies is good (exceeding 0.6) for most months of the year when the anomaly is large. It will be shown in section 4.3 that this correlation is due to a combination of the effect of the equatorial QBO and the IAV in the forcing of the planetary waves at 368K. Note that the model produces a large IAV in the ozone column during polar night (figure 7b), which is when TOMS is unable to measure the ozone column. A high variability during polar night is perhaps not surprising since ozone has a very long chemical lifetime then and will be strongly affected by variability in the dynamics of the NH, which is large during winter.

In the SH at high latitudes the correlation is strong (over 0.6, which is near the 99% significance level) during November, which is the time of greatest ozone column variability there. The modeled variability (figure 7(b)) is less than observed, however. The large

variability observed may be due to the presence in the real atmosphere of the ‘ozone hole’, which is not simulated by the model (since it maintains the chlorine loading representative of 1980). From figure 8 (in which the TOMS data has *not* been detrended) it can be seen that the model’s variability at 70S in November is very similar to that observed until 1985.

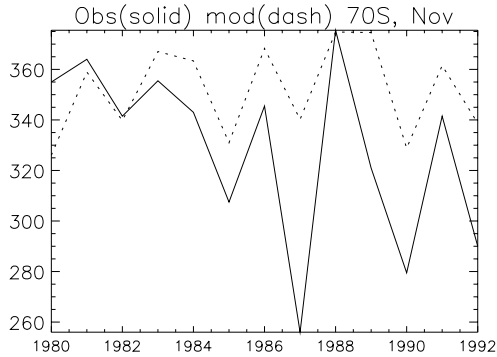


Figure 8: *Non-detrended TOMS (solid) and modeled (dashed) ozone column at 70S in November.*

After 1985 the negative anomalies observed in 1987, 1990 and 1991 have a much stronger negative trend than the more positive anomalies of 1986, 1988 and 1991. This suggests that there is a positive feedback which amplifies the negative anomalies, perhaps in the following way. If the southern pole becomes colder than usual due to the QBO there will be more ozone depletion (if the chlorine loading is high) due to enhanced polar stratospheric cloud formation. This will lead to reduced solar ozone heating, a stronger vortex, a decrease in planetary wave activity and so less in-mixing of ozone from lower latitudes which will further reduce ozone values.

As a comparison with figure 1a, the correlation coefficient between the modeled ozone column anomaly and the 20mb Singapore wind was calculated. In general, the modeled correlations (figure 9) are stronger than observed.

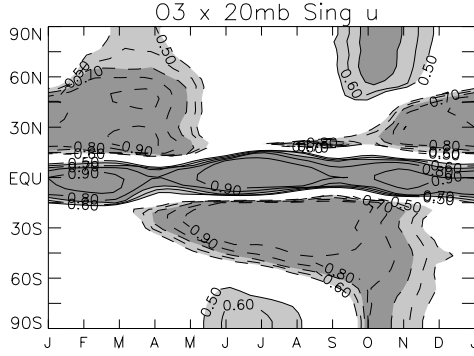


Figure 9: *As figure 1a but using modeled ozone column.*

The anti-correlation of the high-latitude SH anomaly with the 20mb Singapore wind is reproduced, though in the model it is strongest in October, while the observed anti-correlation is strongest in November. Since the equatorial ozone anomaly in the real atmosphere must depend on the zonal wind at all longitudes and over a band of latitudes within about 10 degrees of the equator, and not just on the wind over Singapore, while the modeled ozone is modulated by the Singapore wind, it is not surprising that the model is better correlated than observations with the Singapore wind. Figure 9 does show, though, the regions and times at which the modeled ozone anomaly is very sensitive (with correlations exceeding 0.9) to its 20mb equatorial zonal-mean zonal wind. The model also reproduces the positive correlation seen in figure 1a near 60N in October, which seems (see figure 13 and discussion in section 4.2) to be a remnant of the spring anomaly at 30N. Note also that the correlations at northern high latitudes in spring are lower than those during spring at southern high latitudes. This is because of the added variability in the NH due to the variability in the forcing of planetary waves.

The vertical structure of the ozone variability has been studied using SAGE II data by Zawodny and McCormick (1991), Hasebe (1994) and Randel and Wu (1996). The vertical structure of the standard deviation of the modeled monthly-mean ozone density (in DU/km) from its climatological value is shown in figure 10.

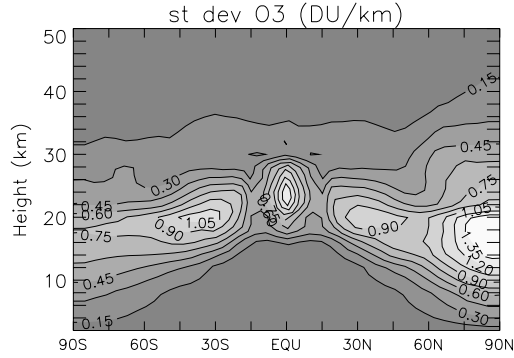


Figure 10: *Standard deviation from the monthly climatology of the modeled ozone density (in DU/km).*

Over the equator between 20 and 30km the variability reaches about 1 DU/km, which is very close to the value observed by Randel and Wu (1996), though between 30 and 35km the value is about a third of that observed. This is due to the model's poor simulation of the upper stratospheric QBO (which will not be described here). At 30N and 30S near 20km there are peaks in the ozone density variability, as observed by Randel and Wu (1996), though the variability near 30km is again less than observed. At high northern latitudes there is a large variability from the troposphere to the middle stratosphere.

As has been pointed out by several authors (eg. Chipperfield et al. (1994), Randel and Wu (1996)) ozone in the middle stratosphere is chemically determined, mainly by the concentration of NO_2 , with larger values of NO_2 causing lower ozone values. As a comparison with Randel and Wu's figure 18, figure 11 here shows the modeled correlation between monthly-mean ozone and NO_2 over all months of the 13 year model run.

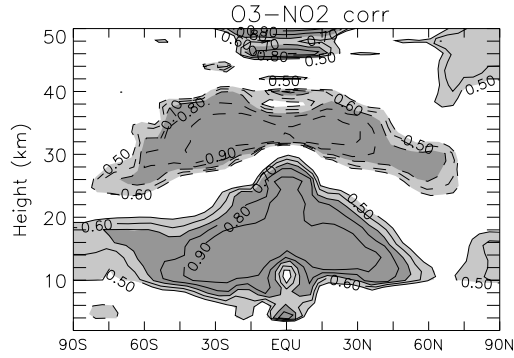


Figure 11: *Correlation of modeled ozone and NO_2 anomalies. Contours and shading as in figure 1.*

This involves 156 months, but if ozone or NO_2 anomalies persist for about 3 months then we estimate about 50 degrees of freedom. In that case, the 99.9% significance level lies at a correlation of 0.4, so it can be seen that there is a strong anti-correlation between NO_2 and ozone over the equator between about 30 and 40km extending polewards to about 60N and 60S between 25 and 30km. The line of zero correlation is plotted on figure 10, from which it can be seen that the majority of the ozone anomaly lies below it in the dynamically controlled (for ozone) region while a smaller part of the anomaly (perhaps a quarter of it) lies in the chemically controlled region. The chemically controlled part is therefore slightly smaller than Randel and Wu's estimate of a third, using the SAGE II data.

4.2 Equatorial QBO-only run

In order to isolate the effect of the equatorial zonal wind, the model was run with the tropical winds relaxed towards the observed Singapore wind, as in the previous run, but with an annually periodic planetary wave forcing at the 368K isentropic surface (using the July 1980 to June 1981 values repeatedly). This is similar to the method used by Gray and Pyle (1989), Gray and Ruth (1993), and Chipperfield et al. (1994).

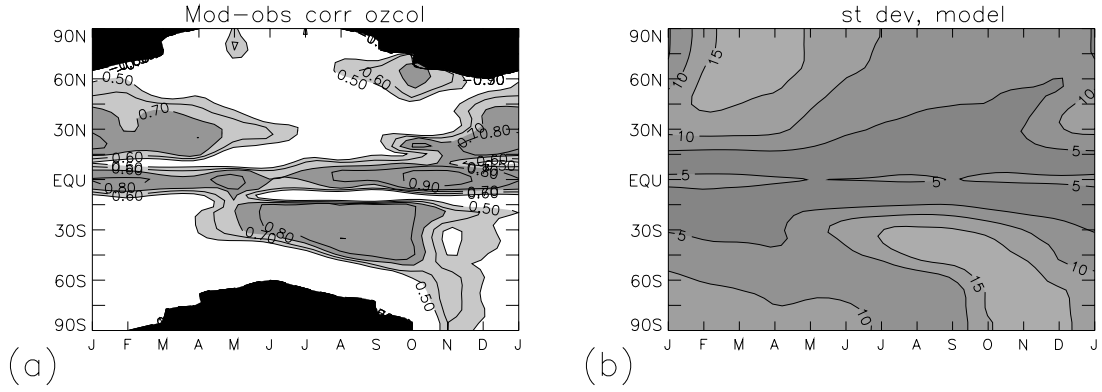


Figure 12: As figure 7 but for model run with variation of equatorial winds only (section 4.2).

The correlation between modeled and observed ozone column (figure 12a) south of about 50N is very similar to that of Run A (figure 7), which shows that the ability of the model to simulate the low and middle latitude (and also the SH November high latitude) ozone anomaly is due to the forcing of the equatorial QBO. North of 50N, but only from September to November, the model is well correlated with observations (as it was in Run A). Thus the QBO does appear to play a part in the high latitude NH ozone anomaly, but only in the autumn. However, this anomaly does not appear to be connected in the usual way to the equatorial wind in autumn – in figure 1a there is a region of *correlation* between the 20mb Singapore wind and the October ozone anomaly at 60N, as opposed to the expected anti-correlation. The anomaly in October appears to be a remnant of the sub-tropical NH spring anomaly, as revealed by figure 13, which shows the correlation of the observed October anomaly at 65N with the anomaly over the preceding 12 months. The sub-tropical spring anomaly appears to persist through summer at low latitudes and then to move polewards during autumn.

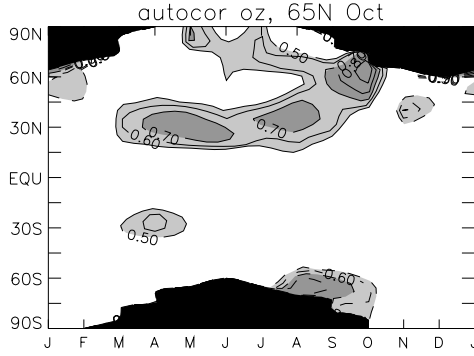


Figure 13: *Correlation of observed ozone column anomaly (detrended and deseasonalised) at 65N in October with observed anomaly at all latitudes over the preceding 12 months. Contours and shading as figure 1.*

The modeled anomaly (figure 12b) is also very similar to that of Run A south of 50N, but farther north the anomaly is much smaller than that of Run A during winter and reaches a maximum in spring of about half the value of Run A.

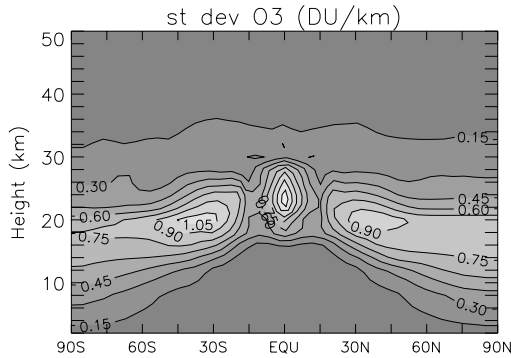


Figure 14: *As figure 10 but for model run with variation of equatorial winds only (section 4.2).*

The vertical structure of the ozone anomaly in this QBO only run (figure 14) is very similar to that of Run A, except at high northern latitudes where the anomaly is smaller in general (about half of the total) and particularly above about 25km. This will be discussed further in the following subsection.

4.3 Run with IAV in forcing of planetary waves only.

In order to isolate the ozone variability due to the varying forcing of planetary waves, a second control run was performed which was identical to Run A except that no equatorial QBO forcing was applied and the model was allowed to calculate its own equatorial winds.

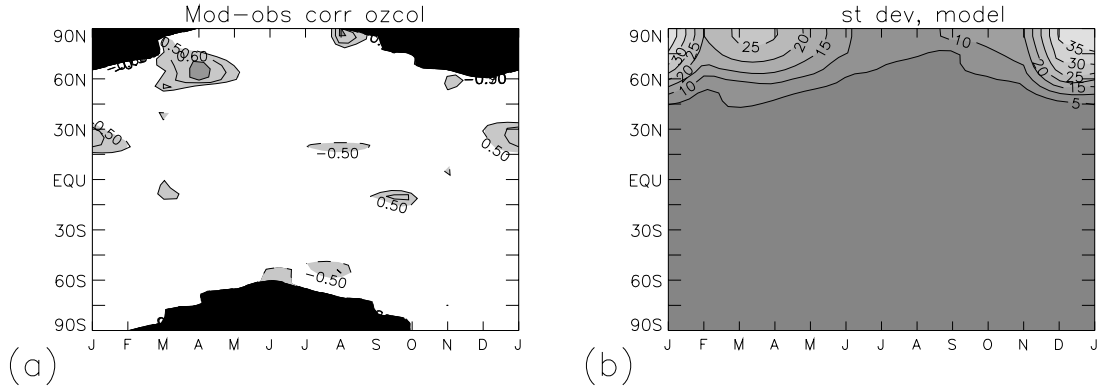


Figure 15: As figure 7 but for model run with year-to-year variation of 368K planetary wave heights only (section 4.3).

The size of the anomaly in the modeled ozone column from this run (figure 15b) is small south of 40N, but north of about 60N it is very similar to that of Run A. The correlation between modeled and observed ozone column (figure 15a) is fairly strong near 60N from March to May and in November, though unfortunately polar night obscures TOMS data in the region where most of the modeled variability lies. Note however that the strong correlations with observations north of 60N in January and February apparent in Run A (figure 7) do not occur in this model run. It seems that the total anomaly is therefore a combination of the anomalies produced by the QBO and the variability in the forcing of planetary waves. This is confirmed by figure 16, in which the anomalies at 65N in February are plotted for all three runs. It can be seen that the good agreement produced by Run A in 1986, for example, is due mainly to the anomaly produced by the planetary wave variability, while in 1987 it is due mainly to the QBO.

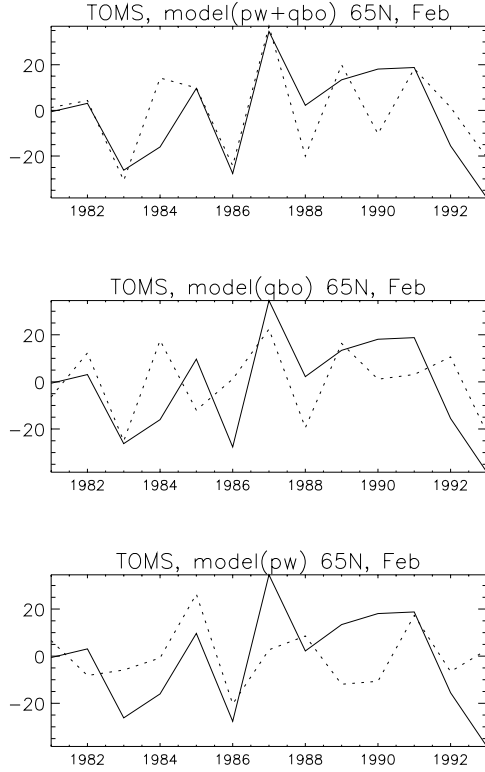


Figure 16: *Observed (solid) and modeled (dashed) ozone column anomalies at 65N in February from (a) Run A, (b) run with variation of equatorial winds only (section 4.2) and (c) run with variation of 368K planetary wave heights only (section 4.3).*

The vertical structure of the anomaly (figure 17) shows that the discrepancy between the anomalies of Run A (figure 11) and the QBO run of section 4.2 (figure 15) is due, not surprisingly, to the variability in the forcing of planetary waves. Figures 14 and 17 show similar values in the high-latitude troposphere, but above 20km the high-latitude anomaly due to variability in the forcing of planetary waves is much larger than that due to the equatorial QBO. This is presumably because the planetary waves affect the high northern latitudes strongly during winter when the high latitude ozone at all heights is dynamically controlled.

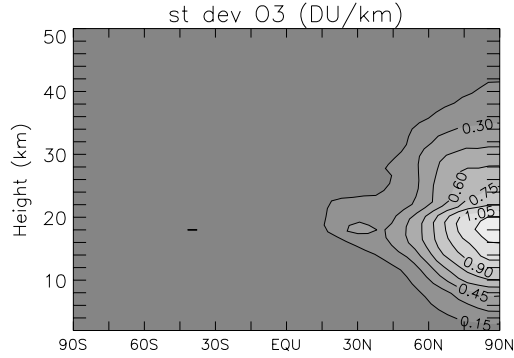


Figure 17: *As figure 10 but for model run with year-to-year variation of 368K planetary wave heights only (section 4.3).*

5 Discussion and Conclusions

It has been shown that much of the ozone variability between about 50N and 50S can be accounted for by the effect of the equatorial winds on the extra-tropical circulation (though a detailed investigation of the mechanism will be described in a later paper). This is consistent with previous observational studies (eg. Randel and Wu (1996)). Observational results shown here suggest that the ozone column anomaly produced in June near 15S propagates southwards past 45S in August to reach the south pole in November. The model shows a similar propagation of the SH sub-tropical autumn anomaly (which is induced mainly by the equatorial 20mb zonal wind) towards the south pole, though it reaches the pole in October, slightly earlier than observed. The model therefore contains a mechanism capable of producing a realistic propagation of the anomaly, and analysis of this mechanism will be presented in a later paper. One striking difference between the modeled and observed anomalies is the rapid growth of the observed SH anomaly (see figure 2) as it nears the south pole, while the modeled anomaly is larger than observed at middle latitudes but maintains a fairly constant amplitude as it nears the pole. The growth of the observed anomaly may be due to the presence in the stratosphere of large concentrations of chlorine after 1985 which may amplify the negative ozone QBO anomalies at high latitudes (see section 4).

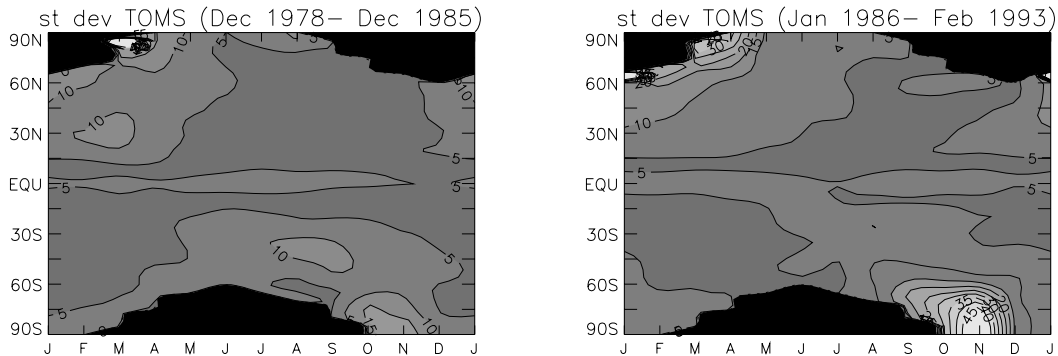


Figure 18: *As figure 2 but (a) from Dec 1978 to Dec 1985 and (b) from Jan 1986 to Feb 1993.*

Figure 18 shows the amplitude of the observed ozone anomaly in the seven years before (figure 18a) and after (figure 18b) January 1986. (Note that the trends have been removed from the data in figures 2 and 18, so they do not contribute to the amplitude of the anomaly). Before 1986 the size of the anomaly in the SH is much closer to that modeled (see figure 7b and note that the chlorine loading in the model is typical of that in 1980) while after 1986 the anomaly over the south pole has increased about three-fold and now reaches a maximum in November as opposed to October. Interestingly, the anomaly in the NH is also larger during the later period, perhaps indicating that a similar process is occurring there. This is an interesting result but obviously far from conclusive.

In the NH, the interannual variability in planetary wave forcing from the lower stratosphere has a large effect on the high latitude ozone column. When both of these forcing terms are included in the model, it is able to reproduce much of the observed year-to-year ozone variability between 1980 and 1992. Interestingly, the model indicates that there is a lot of inter-annual variability in the NH polar night (which is when TOMS is unable to make measurements) due to the variability in the forcing of the planetary waves.

The modeled extra-tropical ozone column anomaly is generally better correlated than observations with the Singapore wind. This is partly because the real atmosphere will not respond only to the zonal wind at a single latitude and longitude (such as over Singapore) but to the zonal wind over a range of latitudes and longitudes, and also because of the influence of other factors such as the solar cycle (eg. McCormack and Hood 1996) and volcanic eruptions (eg. Randel et al. (1996)).

Acknowledgements

This work was supported by the National Science Foundation through grant ATM-9526136, and by the National Aeronautics and Space Administration through grant NAG 5-2802. We would like to thank our three reviewers for their comments.

References

- Butchart N. and J. Austin 1996: On the relationship between the quasi-biennial oscillation, total chlorine and the severity of the antarctic ozone hole. *Quart. J. R. Meteorol. Soc.*, **122** 183–217.
- Bowman K.P., 1989: Global patterns of the quasi-biennial oscillation in total ozone. *J. Atmos. Sci.*, **46**, 3328–3343.
- Chipperfield M.P., L.J. Gray, J.S. Kinnersley and J. Zawodny. 1994: A two-dimensional model study of the QBO signal in SAGE II NO₂ and O₃. *Geophys. Res. Lett.* **21**, 589–592
- Dunkerton, T.J. and M.P. Baldwin 1991: Quasi-biennial modulation of planetary-wave fluxes in the northern hemisphere winter. *J. Atmos. Sci.*, **48**, 1043–1061.
- Garcia R.R. and S. Solomon, 1987: A possible relationship between interannual variability in Antarctic ozone and the quasi-biennial oscillation. *Geophys. Res. Lett.*, **14**, 848–851.
- Gray, L.J. and T.J. Dunkerton, 1990: The role of the seasonal cycle in the quasi-biennial oscillation in ozone. *J. Atmos. Sci.*, **47**, 2429–2451.
- Gray, L.J. and J.A. Pyle, 1989: A two-dimensional model of the quasi-biennial oscillation of ozone. *J. Atmos. Sci.*, **46**, 203–220.
- Gray, L.J. and S. Ruth, 1993: The modeled latitudinal distribution of the ozone quasi-biennial oscillation using observed equatorial winds. *J. Atmos. Sci.*, **50**, 1033–1046.
- Hamilton K., 1989: Interhemispheric asymmetry and annual synchronisation of the ozone quasi-biennial oscillation. *J. Atmos. Sci.*, **46**, 1019–1025.
- Hasebe F. 1984: The global structure of the total ozone fluctuations observed on the time scales of two to several years. *Dynamics of the Middle Atmosphere*, J.R. Holton and T. Matsuno, Eds., D.Reidel, 445–464.
- Hollandsworth S.M., K.P. Bowman and R.D. McPeters 1995: Observational study of the quasi-biennial oscillation in ozone. *J. Geophys. Res.*, **100**, 7347–7361.
- Holton J.R. and H.-C. Tan 1982: The Quasi-biennial oscillation in the northern hemisphere lower stratosphere. *J. Meteor. Soc. Japan*, **60** 140–147.
- Holton J.R. and C. Mass, 1976: Stratospheric vacillation cycles. *J. Atmos. Sci.*, **33** 2218–2225.
- Kinnersley, J.S., 1998: Interannual variability of stratospheric zonal wind forced by the Northern lower-stratospheric large-scale waves. *Accepted by J. Atmos. Sci.*
- Kinnersley, J.S., 1996: The Climatology of the stratospheric ‘THIN AIR’ model. *Quart. J. R. Meteorol. Soc.*, **122**, 219–252.

- Kodera K. 1991: The solar and equatorial QBO influences on the stratospheric circulation on the stratospheric circulation during the early northern hemispheric winter. *Geophys. Res. Lett.*, **18**, 1023–1026.
- Kodera K. 1993: Quasi-decadal modulation of the influence of the equatorial quasi-biennial oscillation on the north pole stratospheric temperatures. *J. Geophys. Res.*, **98**, 7245–7250.
- Lait L.R., M.R. Schoeberl and P.A. Newman 1989: Quasi-biennial modulation of the Antarctic ozone depletion. *J. Geophys. Res.*, **94**, 11559–11571.
- McCormack, J.P. and L.L. Hood 1996: Apparent solar cycle variations of upper stratospheric ozone and temperature: Latitude and seasonal dependences. *J. Geophys. Res.*, **101**, 20933–20944.
- Randel W.J. and J.B. Cobb 1994: Coherent variations of monthly mean total ozone and lower stratospheric temperature. *J. Geophys. Res.*, **99**, 5433–5447.
- Randel W.J., F. Wu, J.M. Russell III, J.W. Waters and L. Froidevaux 1995: Ozone and temperature changes in the stratosphere following the eruption of Mount Pinatubo. *J. Geophys. Res.*, **100**, 16753–16764.
- Randel W.J. and F. Wu 1996: Isolation of the ozone QBO in SAGE II data by singular-value decomposition. *J. Atmos. Sci.* **53**, 2546–2559.
- Sitnov S.A. 1996: Vertical structure of the extratropical quasi-biennial oscillation in ozone, temperature, and wind derived from ozonesond data. *J. Geophys. Res.*, **101**, 12855–12866.
- Tung K.K, and H. Yang 1994a: Global QBO in circulation and ozone. Part I: Reexamination of observational evidence. *J. Atmos. Sci.*, **51** 2699–2707.
- Tung K.K, and H. Yang 1994b: Global QBO in circulation and ozone. Part II: A simple mechanistic model. *J. Atmos. Sci.*, **51** 2708–2721.
- Yang, H., K.K. Tung and E.P. Olaguer, 1990: Nongeostrophic theory of zonally averaged circulation. Part II: Eliassen-Palm flux divergence and isentropic mixing coefficient. *J. Atmos. Sci.*, **47**, 215–241.
- Yang, H. and K.K. Tung 1995: On the phase propagation of extratropical ozone quasi-biennial oscillation in observational data. *J. Geophys. Res.*, **100**, 9091–9100.

Figure captions

Figure 1:

Figure 2:

Figure 3:

Figure 4:

Figure 5:

Figure 6:

Figure 7:

Figure 8:

Figure 9:

Figure 10:

Figure 11:

Figure 12:

Figure 13:

Figure 14:

Figure 15:

Figure 16:

Figure 17:

Figure 18: